

# Physical mapping of the human pseudo-autosomal region; comparison with genetic linkage map

Christine Petit, Jacqueline Levilliers and Jean Weissenbach

Unité de Recombinaison et Expression Génétique, INSERM U-163, CNRS UA-271, Institut Pasteur, 28 rue du Dr Roux, 75015 Paris, France

Communicated by J. Weissenbach

**A long-range restriction map of the pseudo-autosomal or exchange pairing region (corresponding to the terminal parts of the short arms of the human sex chromosomes) has been established using pulsed field gel electrophoresis. A total of seven loci have been located on this physical map based essentially on the analysis of 45,X Turner genomes. The region spans a total of 2600 kb. The 5' end of the MIC2 gene maps at <80 kb from the proximal pseudo-autosomal boundary. Since the total pseudo-autosomal linkage interval represents ~50% of recombination at male meiosis, 1 cM corresponds to 50–60 kb. This is consistent with the almost 20-fold increase in recombination frequency observed in male versus female meiosis in this region. The present data show no distortion between both physical and linkage maps. The distribution of the CpG-rich restriction sites is notably disequibrated. A large subset of these sites is concentrated within the 500 kb closest to the telomere whereas others appear in clusters (probably HTF islands) scattered in the rest of the pseudo-autosomal region.**

**Key words:** human genome mapping/human sex chromosomes/pseudo-autosomal region/telomere

## Introduction

Mammalian X and Y chromosomes share a small region of strictly homologous DNA sequences. This region is located at one tip of the sex chromosomes (Singh and Jones, 1982; Evans *et al.*, 1982; Buckle *et al.*, 1985; Cooke *et al.*, 1985; Simmler *et al.*, 1985; Weber *et al.*, 1987). In man it represents the distal end of the X–Y pairing region which extends to a variable amount of the short arms of the X and Y chromosomes (Chandley *et al.*, 1984). Loci from this region can be exchanged between both sex chromosomes through a crossing over during male meiosis and therefore show either partial or no sex linkage (Cooke *et al.*, 1985; Keitges *et al.*, 1985; Simmler *et al.*, 1985). This autosomal-like mode of segregation has been termed pseudo-autosomal (Burgoyne, 1982).

Existence of a pseudo-autosomal region has been shown using formal genetics and DNA analysis in mouse (Keitges *et al.*, 1985; Harbers *et al.*, 1986), and by DNA analysis only, in man (Cooke *et al.*, 1985; Simmler *et al.*, 1985) and chimpanzee (B. Weber *et al.*, submitted).

Genes from this region are present in two doses in both sexes and should thus escape inactivation on the X chromo-

some (Lyon, 1963). This has indeed been observed for MIC2, the only pseudo-autosomal gene known to date (Goodfellow *et al.*, 1984). It has also been postulated that somatic defects associated with Turner's syndrome are caused by the absence of either Y-linked genes or a copy of non-inactivated X-linked genes (Ferguson-Smith, 1965; Burgoyne, 1982), possibly from the pseudo-autosomal region.

Several unusual properties, apparently differing among species, characterize the pseudo-autosomal region. Segregation analyses have shown that double recombinations (Keitges *et al.*, 1987; Soriano *et al.*, 1987) and unequal cross-overs (Harbers *et al.*, 1986) are rather frequent in mouse. In contrast, no double event has been observed in human family analyses to date (Darling *et al.*, 1986; Rouyer *et al.*, 1986b; Page *et al.*, 1987). A 10- to 20-fold increase in recombination frequency is observed in human male versus female meiosis (Rouyer *et al.*, 1986b). Assuming an obligatory crossing over between each chromosomal pair at meiosis (Koller and Darlington, 1934) this would have to take place within the pseudo-autosomal region in males. On the other hand this event could occur at any location(s) on the female X chromosomes and only occasionally in the pseudo-autosomal part, provided that the size of this region is small.

Mapping of the proximal boundary of the pseudo-autosomal region within a small interval was a fulfilled prerequisite for sizing the region (Pritchard *et al.*, 1987). Because of its very high recombinogenic activity in male meiosis, the pseudo-autosomal region is a privileged area for a structural analysis of homologous recombination in mammals. A comparison of physical and recombination distances represents a first step in this respect. In addition, a physical mapping of the pseudo-autosomal region using pulsed field electrophoretic procedures may help to localize HTF islands corresponding to putative genes (Bird, 1986) possibly involved in the appearance of Turner stigmata. We therefore established a long-range restriction site map of the telomeric part of the X and Y chromosome short arms including seven pseudo-autosomal loci.

## Results

Data have been collected from peripheral blood lymphocytes from five 45,X Turner individuals. The map has been derived from values from a single case. Linking and ordering of the restriction fragments is based on their simultaneous detection by different probes using 'total' or partial digestions. More accurate localizations were obtained by double digestions. Positions are indicated in kilobase coordinates starting from the telomere as follows: pte1:450 means 450 kb from Xp and Yp telomeres. For convenience, restriction fragments detected by a probe are designated in brackets by the relevant locus name followed by the abbreviation(s) of the restriction enzyme(s) used to generate this fragment;

**Table I.** Sizes (kb) of restriction fragments determined by Southern blot hybridization of PFG

	(A) Fragments detected with probe 362A	(B) Fragments detected with probe U7A	(C) Fragments resulting from double digestions detected with probe U7A
<i>ClaI</i>	360, (430), 530 <sup>a</sup>	360, (430), 530 <sup>a</sup>	<i>BssHII</i> + <i>NruI</i> 270
<i>MluI</i>	250, 290, (360), (410), (460), 490, 520 <sup>a</sup>	(60), (100–140), 210, 240, (360), (410), (460), 490, 520 <sup>a</sup>	<i>NorI</i> + <i>NruI</i> 220
<i>SaII</i>	(30), (110), (120), (160), 520 <sup>a</sup> , 540 <sup>b</sup>	520 <sup>a</sup> , 540	<i>SfiI</i> + <i>NorI</i> 220
<i>NruI</i>	180, 210	270, 300	<i>SfiI</i> + <i>NruI</i> 220
<i>NruI</i> partial	180, 210, 480, 510	270, 300, 480, 510	<i>SfiI</i> + <i>XhoI</i> 220
<i>NorI</i>	(70), 130	220, 270	<i>BssHII</i> + <i>NorI</i> 220
<i>NorI</i> partial	130, (210), (260), (480), 510 <sup>c</sup>	220, 270, 380, 480, 510	
<i>BssHII</i>	140, 160	290	
<i>BssHII</i> partial	140, 160, 210, 500	290, 340, 500	
<i>SacII</i>	(50), 70, (100)	290	
<i>SacII</i> partial	70, (100), 210, 500		
<i>NarI</i>	(70), 80, (100), 140, (210)	290	
<i>NarI</i> partial	80, 140, 210, 500		
<i>NaeI</i>	(40), (60), (90), 140, 160		
<i>XhoI</i>	(80), (100), 130	250	
<i>XhoI</i> partial	(80), (100), 130, 230, 480, 510		
<i>SfiI</i>	40, 60	270	
<i>SfiI</i> partial	40, 60, (100), (130), (150)		
<i>EagI</i>	(30), (40), (70), (130)	80	
<i>EagI</i> partial	(30), (40), (70), (130), (210), (260), (310), (400), (480), (510)		

Weak bands are indicated by parentheses.

<sup>a</sup>Several fragments differing by 10–20 kb could be occasionally detected.

<sup>b</sup>Additional *SaII* fragments of 230, 260 and 430 kb were observed in some 45,X individuals.

<sup>c</sup>Additional *NorI* fragments of 310, 370 and 400 kb were observed in some 45,X individuals.

e.g. [DXYS17 *NorI* + *SaII*] designates a restriction fragment hybridizing to probe 601 obtained after double digestion by *NorI* + *SaII*.

#### Linking DXYS60 to the telomere

The telomeric probe 362A (locus DXYS20) is located at a distance of 20–30 kb proximal to the Xp/Yp extremity (see Materials and methods). In nine out of 12 different restriction digests, fragments < 210 kb were detected with 362A (Table I). These fragments were not observed with probe U7A (locus DXYS60). The three other enzymes, *ClaI*, *MluI* and *SaII*, produce telomeric fragments scattered up to 500 kb. Those between 360 and 500 kb hybridize to U7A, whereas those < 290 kb do not (Figure 1). This locates DXYS60 between p<sub>tel</sub>:290 and p<sub>tel</sub>:360. Partial digestions with the nine former enzymes were probed with 362A and U7A (Table I). The data obtained allow the construction of a detailed sub-regional restriction map of the most distal 500 kb (Figure 2) and confirm the location of DXYS60. Double digestions allow the mapping of an *SfiI* site at p<sub>tel</sub>:260. Numerous individual variations were reproducibly observed with *NorI* and *SaII* and are the result of additional sites observed in some of the 45,X Turner patients.

#### Linking DXYS28 to the telomere

Probe pDP411 (locus DXYS28) detects fragments of ~5–30 kb in all 'complete' digests tested (Figure 3) and one or two additional larger fragments, in *NorI*, *SaII*, *MluI*, *XhoI* and *SfiI* (Table II) and *ClaI* (not shown). DXYS28 is included in a region displaying a very high density of undermethylated CpG doublets. The large [DXYS28 *SaII*],

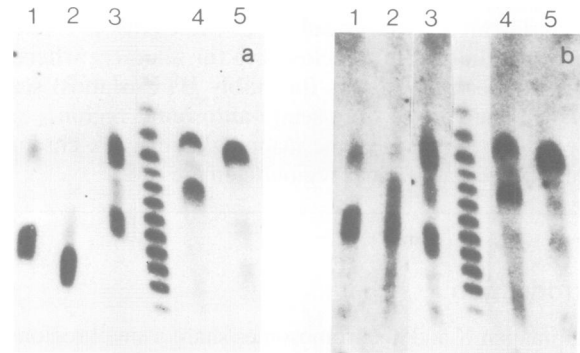


**Fig. 1.** PFG analysis of 45,X peripheral lymphocytes probed for loci DXYS20 and DXYS60. Products of partial restriction digestions by *NruI* (lane 1), *NorI* (lane 2) and total restriction digestions by *MluI* (lane 3), *ClaI* (lane 4) and *SaII* (lane 5) were probed with 362A (a), U7A (b) and  $\lambda$  DNA (a and b). The lowest marker band corresponds to  $\lambda$  monomer (48.5 kb).

[DXYS28 *MluI*], [DXYS28 *ClaI*] fragments (520–540 kb) hybridize also to 362A and to U7A. However, the [DXYS28 *NorI*] (800-kb) fragment, though larger than 540 kb, does not and extends therefore proximal to DXYS28. Since pDP411 detects only small fragments of  $\leq$  30 kb in a double *NorI* + *SaII* digest, DXYS28 maps at p<sub>tel</sub>:510–520. The CpG-rich region including DXYS28 is framed by a totally cleavable *NorI* site at p<sub>tel</sub>:510 and by partially resistant ones around p<sub>tel</sub>:530. *NorI* digestion of other partial digests will thus create an end hybridizing to pDP411 and allow a proximal extension of the map (see below).

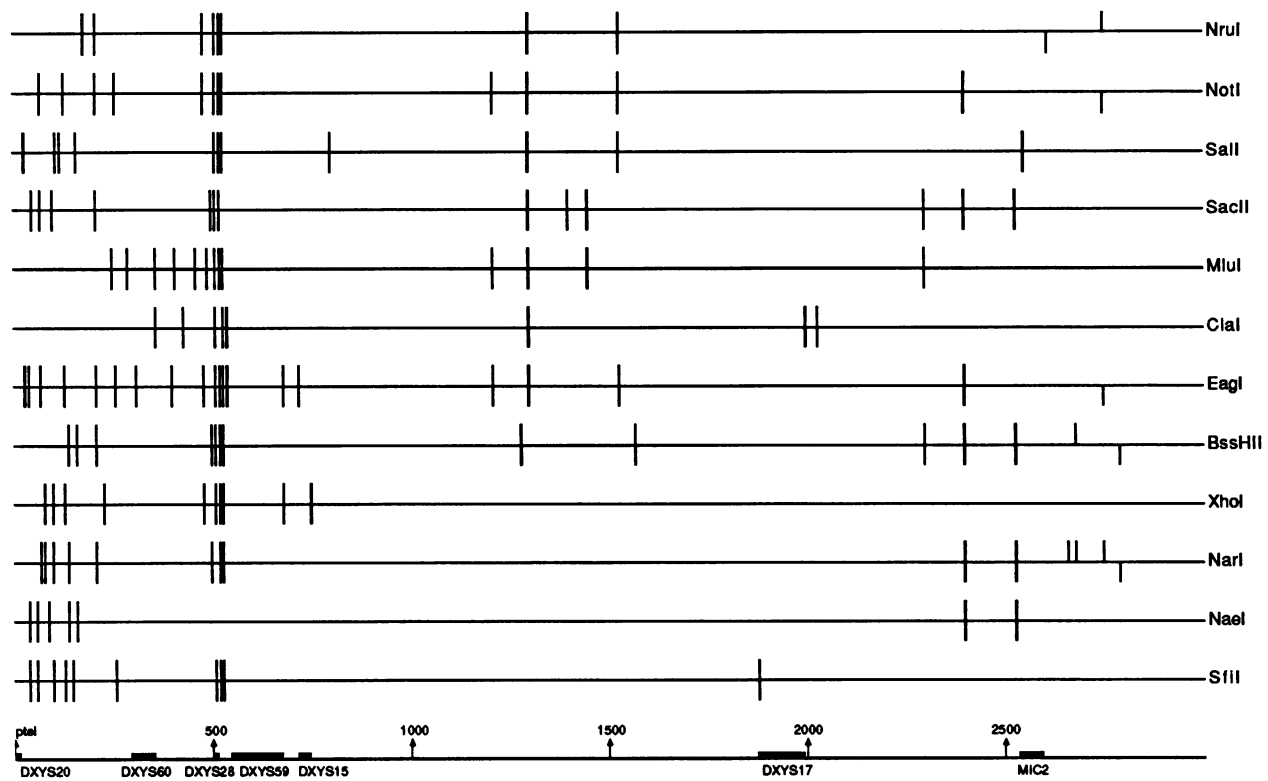


**Fig. 2.** Long-range restriction map of the human pseudo-autosomal region. The data for producing this map are extracted from Tables I–IV and from double digestions reported in Results. Major and reproducibly observed pseudo-autosomal sites for *NruI*, *NotI*, *SacII* and *BssHII* have been positioned on this map. Only a subset of the restriction sites for the other enzymes are represented. Pseudo-autosomal sites are represented by vertical bars crossing the horizontal lines. Chromosome-specific sites are represented by vertical bars extending only above the line when X-located and below the line when Y-located. Coordinates indicate distances in kilobases from X and Y short arm telomeres. Restriction sites located within a 30- to 40-kb interval around ptel:520 were too numerous to be accurately positioned. Intervals of loci localization are indicated by the horizontal solid bars on the lowest line. Beyond ptel:540, clusters of restriction sites (three sites at least) appear at ptel:1300, ptel:1530, ptel:2300, ptel:2400 and ptel:2530 (MIC2 HTF island).

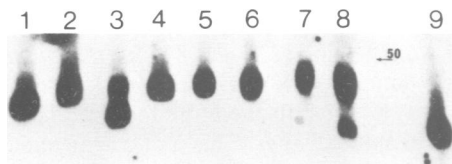


**Fig. 3.** PFGE analysis of 45,X peripheral lymphocytes probed for locus DXYS28. Products of total restriction digestions by *NorI* (lane 1), *ClaI* (lane 2), *Sall* (lane 3), *NaeI* (lane 4), *BssHII* (lane 5), *NruI* (lane 6), *SacII* (lane 7), *EagI* (lane 8) and *NarI* (lane 9) were probed with pDP411. All bands detected are < 50 kb.

#### Linking DXYS28 to DXYS15 and DXYS59

A *NorI* fragment of 800 kb and an *XhoI* fragment of 240 kb are simultaneously detected by probes pDP411 (DXYS28), 68A (DXYS59) and 113D (DXYS15). However, a major *XhoI* fragment (170 kb) hybridizes only to pDP411 and 68A (Table II). This indicates that DXYS15 is proximal to DXYS59 and DXYS28. Data obtained using the artificial end generated by *NorI* at DXYS28 (see above) support this conclusion. A *NorI* digestion of a partial *EagI* digest produces two fragments of 160 kb and 210 kb detected by pDP411 and 68A but not by 113D. Similarly, on a partial *Sall* digest, a *NorI* digestion produces a fragment of 300 kb detected by pDP411, 68A and 113D. These results place DXYS59 between ptel:530 and ptel:670 and DXYS15 between ptel:720 and ptel:750.

Additional data relevant to the region proximal to DXYS28 were obtained with *Sall*, *BssHII*, *NruI*, *MluI* and *SacII* (Table II). All these single digestions produce a ~770-kb fragment detected by 68A and 113D. This large fragment is not shortened by a second *NorI* cleavage, indicating that these sites are clustered on each end of these 770-kb fragments, probably in HTF islands. Since the [DXYS59–DXYS15 *NorI*] fragment is also partially linked to DXYS28 (see above), the distal island corresponds to the CpG-rich region at ptel:530 and hence the proximal island maps at ptel:1300. Indirect end labelling of partial *NorI*, *NruI*, *SacII* and *Sall* digestions by probe 362A confirms the existence of this ptel:1300 CpG island. 68A detects a minor *SacII* fragment of 870 kb (Table II) and as mentioned above a *Sall* fragment of 870 kb in some individuals (Table II, Figure 4). These fragments are not revealed by pDP411 and thus extend on the proximal side. When submitted to a second digestion with *NorI* these two fragments are reduced to 770 kb and therefore map between ptel:530 and ptel:1400. *NruI* and *NorI* digestions both yield a 1000-kb fragment detected by 68A. This *NorI* fragment remains practically unchanged after *NruI* digestion (Figure 4). Again the *NruI* fragment does not contain DXYS28 and thus both proximal *NruI* and *NorI* sites map at ptel:1530.

#### Linking DXYS17 to MIC2

When probed with 601 (DXYS17) *Sall* and *NruI* digests show two major fragments of 1020 and 1220 kb respectively.

**Table II.** Sizes (kb) of restriction fragments determined by Southern blot hybridization of PFG

	<i>NotI</i>	<i>NruI</i>	<i>SalI</i>	<i>BssHII</i>	<i>MluI</i>	<i>SacII</i>	<i>SfiI</i>	<i>EagI</i>	<i>NaeI</i>	<i>XhoI</i>
pDP411	~ 10 ~ 20 ~ 30 (800)	~ 10 ~ 30	~ 10 ~ 20 ~ 30 (520) (540)	~ 10 ~ 20 ~ 30	~ 5 ~ 20 ~ 30 (520)	~ 20 ~ 30	(~ 20) (~ 30) 270	~ 10 ~ 20 ~ 30	~ 20 ~ 30	~ 10 ~ 20 ~ 30 170 (240)
68A	(680) 770–800 (1000)	770 (1000)	270 300 770 <sup>a</sup>	750	100 150 680 (770)	770 (870)	130	140 190	(180) (190)	150 170 (240)
113D	(680) 770–800 (1000)	770 (1000)	270 300 770 <sup>a</sup>	750	530 680 (770)	770 (870)	140	510	70 (180) (190)	70 (240)

Weak bands are indicated in parentheses.

<sup>a</sup>Replaced by a 870-kb fragment in some 45,X individuals; both the 770-kb or 870-kb fragments can be accompanied by an additional fragment of ~600 kb.

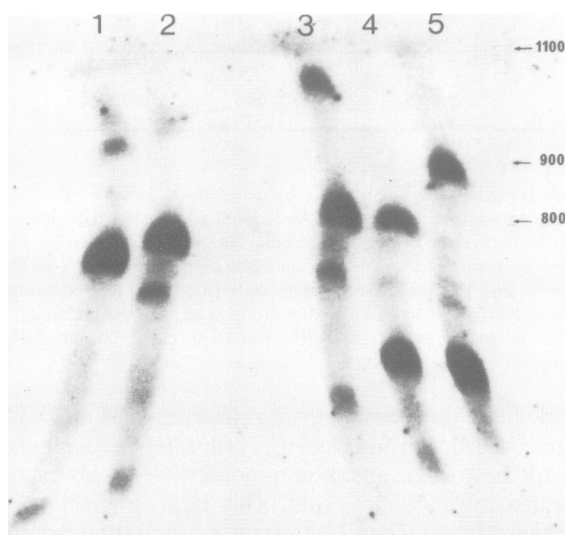


**Fig. 4.** PFG analysis of 45,X peripheral lymphocytes probed for locus DXYS59. Products of restriction digestions by *NruI* (20 U) (lane 1), *NotI* (2 U) (lane 2), *SalI* (20 U) (lane 5), *NotI* (2 U) + *NruI* (20 U) (lane 3), *NotI* (2 U) + *SalI* (20 U) (lane 4) were probed with 68A.

On partial digestion, 601 also detects an additional weak *NruI* fragment ~1450 kb and an additional minor *SalI* fragment of 1150 kb (Table III). All these *NruI* and *SalI* fragments hybridize also to p44C and 19B (locus MIC2). Probe 601 detects large *NotI*, *BssHII*, *MluI*, *Clal* and *SacII* fragments (Table III) which do not hybridize to MIC2 probes.

Data obtained from double digestions were used to derive a restriction map of this sub-region (Table III) which was oriented according to the recombination map placing DXYS17 distal to MIC2 (Rouyer *et al.*, 1986b; Goodfellow *et al.*, 1986). [DXYS17 *NotI*], [DXYS17 *NruI*], [DXYS17 *BssHII*], [DXYS17 *SalI*], [DXYS17 *MluI*] and [DXYS17 *SacII*] fragments were shortened when submitted to *Clal* digestion, and the resulting fragments were always unique and inferior to [DXYS17 *Clal*] (Figure 5a). These single digest fragments therefore overlap one side of the 680-bp [DXYS17 *Clal*] fragment. Since none of the *SalI* + *Clal* and *NruI* + *Clal* double digest products (450 kb) hybridizes

simultaneously to 601 and MIC2 probes, the proximal end of [DXYS17 *Clal*] is at 450 kb from the distal end of both the [DXYS17 *NruI*] and [DXYS17 *SalI*] fragments. Double digestions including *Clal* also allow the location of the distal ends of [DXYS17 *NotI*], [DXYS17 *BssHII*], [DXYS17 *MluI*] and [DXYS17 *SacII*] (Figure 5b and Table III). The distal *NotI*, *NruI* and *SalI* sites are clustered at 450 kb distal to [DXYS17 *Clal*], while *MluI* and *SacII* are at 530 kb and *BssHII* at 410 kb from [DXYS17 *Clal*]. Data from double digestions with *NotI*, *NruI* and *SalI* are all consistent with this result. A more accurate mapping of DXYS17 was derived from the double *SfiI* + *Clal* digestion which produces a [DXYS17 *SfiI* + *Clal*] fragment of 120 kb (Table III).

The distal ends of [DXYS17 *SalI*], [DXYS17 *NruI*] and [DXYS17 *NotI*] (1020, 1220 and 870 kb respectively) are in a cluster; but only [DXYS17 *SalI*] and [DXYS17 *NruI*] hybridize to 19B. MIC2 is therefore localized between the proximal *NotI* and *SalI* sites. This *SalI* fragment occurs on both the X and Y chromosomes, but the *NruI* fragment is sex chromosome specific. Pritchard *et al.* (1987) have already positioned a *SalI* site closely proximal (<20 kb) to the 5' end of MIC2. This 5' end of the gene is characterized by an HTF island composed of *SacII*, *NaeI*, *NarI* and *BssHII* sites (Pritchard *et al.*, 1987). *SalI* + *NarI* and *SalI* + *BssHII* double digestions both produce a 20-kb fragment detected by 19B (Table IV) which spans the 20 kb between the MIC2 HTF island and the closely proximal *SalI* site. This latter site therefore corresponds to the proximal end of the [DXYS17 *SalI*] fragment of 1020 kb. It follows that the distance from DXYS17 to the MIC2 HTF island is between 550 and 670 kb (Figure 2).

Probe p44A (immediately distal to the MIC2 HTF island) detects *BssHII*, *NarI* and *NaeI* fragments of 130 kb each, indicating that their distal ends cluster in another HTF island. [MIC2 *NruI* + *NotI*] is an X-specific fragment of 350 kb which represents the size difference between the single *NruI* and *NotI* digestion products detected by 601 (Table IV). Similarly, *SalI* + *NotI* double digestion produces a fragment of 150 kb also detected by p44A and 19B which again corresponds to the size difference between the single digestion products (Table IV). The proximal site of [DXYS17

**Table III.** Sizes (kb) of restriction fragments containing DXYS17 as determined by Southern blot hybridization of PFG

	<i>NruI</i>	<i>SaII</i>	<i>NotI</i>	<i>BssHII</i>	<i>MluI</i>	<i>Clal</i>	<i>SacII</i>	<i>SfiI</i>
	1220 <sup>a</sup> (~1450) <sup>b</sup>	1020 (1150) <sup>b</sup>	870 (1100) <sup>b</sup>	720	850	(200) (300) 680, 710	850, 950	(30) 240, 310 (390) (410)
+ <i>Clal</i>	450	450	450	410	530		530	(30), 120
+ <i>NotI</i>	870	870		720		450		
+ <i>NruI</i>		1020	870	720		450	770, 870	
+ <i>SaII</i>	1020		870	720				

Weak bands are indicated in parentheses.

<sup>a</sup>An additional fragment of 1070 kb is seen in 46,XY and 49,XYYYY genotypes and shows a Y-linked dosage.

<sup>b</sup>Product observed in partial digests only.

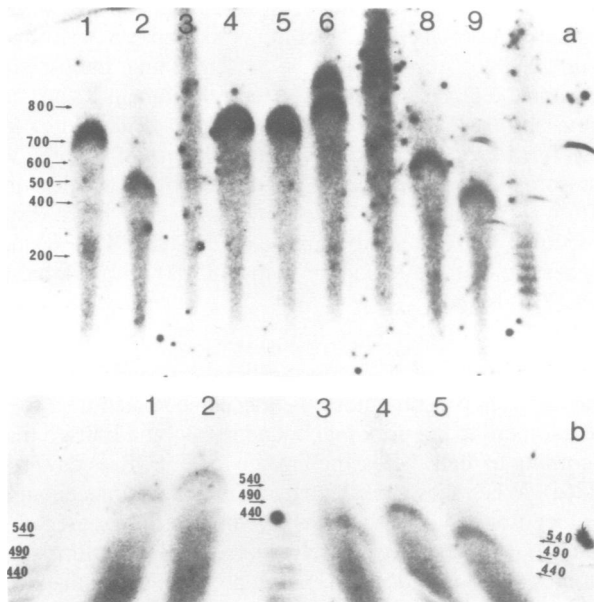


**Fig. 5.** PFG analysis of 45,X peripheral lymphocytes probed for locus DXYS17. (a) Products of total restriction digestions by *Clal* (lane 1), *NruI* + *Clal* (lane 2), *NruI* (lane 3), *BssHII* (lane 4), *BssHII* + *NotI* (lane 5), *SacII* + *NruI* (lane 6), *SacII* (lane 7), *SacII* + *Clal* (lane 8) and *BssHII* + *Clal* (lane 9) were probed with 601. (b) Products of total double digestions by *Clal* + *MluI* (lane 1), *Clal* + *SacII* (lane 2), *Clal* + *BssHII* (lane 3), *Clal* + *SalI* (lane 4) and *Clal* + *NotI* (lane 5) probed with 601.

*NotI*] therefore maps within the HTF island 130 kb distal to the MIC2 HTF island.

#### Joining the telomeric and proximal parts

An *NruI* fragment of 230 kb has been identified between p<sub>tel</sub>:1300 and p<sub>tel</sub>:1530 (Figure 4) (see above). Probe 601 can also detect two large *NruI* fragments also differing by 230 kb (Table III). Though these [DXYS17 *NruI*] fragments are sex chromosome specific, the same difference of 230 kb between these two large fragments is found on each chromosome. It is therefore very likely that the 230-kb *NruI* fragment is pseudo-autosomal and hence distal to the [DXYS17 *NruI* + *Clal*] fragment of 450 kb. To test if this latter *NruI* fragment can be superimposed to that mapping between p<sub>tel</sub>:1300 and p<sub>tel</sub>:1530 we probed a partial *NruI* digest with 362A. This probe allows the detection of fragments up to 4 Mb in a partial *NruI* digest from 48,XXXX and 49,XYYYY DNAs (Figure 6). The following fragments could clearly and reproducibly be observed with 362A: two

**Table IV.** Sizes (kb) of restriction fragments determined by Southern blot hybridization of PFG: (A) restriction fragments detected by probe p44A; (B) restriction fragments detected by probe p19B

(A)	<i>NruI</i>	<i>SaII</i>	<i>NotI</i>	<i>BssHII</i>	<i>NarI</i>	<i>NaeI</i>
	1220 <sup>a</sup> (~1450) <sup>b</sup>	1020 (1150) <sup>b</sup>	(320) <sup>c</sup>	130	130	130
+ <i>NotI</i>				130	130	
+ <i>NruI</i>		150	(320) <sup>d</sup>			
+ <i>SaII</i>		1020	350	130		
			150	130	130	
(B)	<i>NruI</i>	<i>SaII</i>	<i>NotI</i>	<i>BssHII</i>	<i>NarI</i>	<i>SfiI</i>
	1220 <sup>a</sup> (~1450) <sup>b</sup>	1020 (1150) <sup>b</sup>	(320) <sup>c</sup>	150	(130)	20
+ <i>NotI</i>			~1100		150	35
					(220)	140
+ <i>NotI</i>		150		150	(130)	
					150	
+ <i>NruI</i>			(320) <sup>d</sup>		(220)	20
		1020	350	150		35
				(220)		140
+ <i>SaII</i>			150	20	20	

Weak bands are indicated in parentheses.

<sup>a</sup>An additional fragment of 1070 kb is observed in 46,XY and 49,XYYYY genotypes and shows a Y-linked dosage.

<sup>b</sup>Product observed in partial digests only.

<sup>c</sup>An additional fragment of 350 kb is observed in 46,XY and 49,XYYYY genotypes and shows a Y-linked dosage.

<sup>d</sup>An additional fragment of 210 kb is observed in 46,XY and 49,XYYYY genotypes and shows a Y-linked dosage.

strong bands up to 500 kb, one band at 1300 kb, one band at ~1500 kb and a weaker band framed by the 2.1-Mb and 3.2-Mb markers. These results indicate that a single *NruI* fragment of ~200 kb is flanked by two large fragments. It thus appears that the order of the *NruI* sites is as hypothesized above, i.e. p<sub>tel</sub>:1300, p<sub>tel</sub>:1530, Yp<sub>tel</sub>:2600 and Xp<sub>tel</sub>:2750. This conclusion is also sustained by data from partial *NotI* digestions. Similarly to *NruI* and for identical reasons (see above), a *NotI* fragment of 230 kb is located proximal to DXYS59 and distal to DXYS17 (Tables III and IV). The *NotI* and *NruI* clustered sites at p<sub>tel</sub>:1530 thus correspond to the *NruI*, *NotI* and *SaII* site cluster at the distal end of [DXYS17 *NotI*] and [DXYS17 *NruI*]. The distal end of the 680-kb [DXYS17 *Clal*] fragment thus coincides with the CpG site cluster at p<sub>tel</sub>:1300. These results also locate the proximal pseudo-autosomal boundary distal to the Y-specific *NruI* site close to Yp<sub>tel</sub>:2600, i.e. ~70 kb proximal to the MIC2 HTF island. Detection of a [MIC2 *NruI* + *NotI*] Y-specific fragment of 210 kb confirms these

results and allows a more accurate mapping of the Y-specific *NruI* site 80 kb proximal to the MIC2 HTF island.

**Discussion**

**Sizing the human pseudo-autosomal region**

This paper reports the construction of a long-range restriction map of the human pseudo-autosomal region. Two

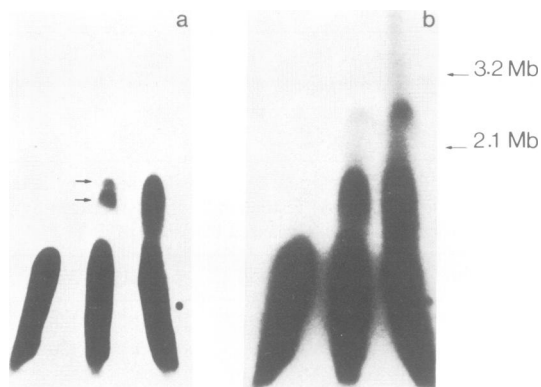


**Fig. 6.** PFG analysis of 48,XXX peripheral lymphocytes by indirect end labelling of locus DXYS20. (a) and (b) are two autoradiographs of the same hybridization at different exposure times. Partial *NruI* digests with decreasing amounts of enzyme from left to right probed by 362A. Arrows indicate the two *NruI* fragments at ~1300 and ~1500 kb.

**Table V.** Correspondence between physical and recombination distances

Interval	kb	Recombinants/ meioses	$\theta$ (%)	Mean distance per cM (kb)
DXYS17-PPB	630	18/145	12.4	51
	750			60
DXYS28-PPB	2090	68/179	38	55
DXYS14-PPB	2610	172/363	47.4	55
DXYS14-DXYS28	520	14/143	9.8	53
DXYS14-DXYS17	1860	45/145	31	60
	1980			64

PPB: proximal pseudo-autosomal boundary is taken as equivalent to the X-Y recombination limit. DXYS17 maps within a broad interval and physical distances corresponding to each extremity of this interval have been taken into account.

separate blocks of overlapping fragments could be derived at the distal and proximal ends. The distal block (1530 kb) ends on its proximal side with a *NruI* fragment of 230 kb. The proximal block (1500 kb) contains on both the X and Y chromosomes an *NruI* fragment of 230 kb that we considered pseudo-autosomal and hence located at the distal end of this block. The two blocks could overlap by this *NruI* fragment. Data from indirect end labelling of a partial *NruI* digestion by hybridization with 362A support this hypothesis. Data from partial *NotI* digestion are also consistent with this map. It follows that the size of the pseudo-autosomal region is between 2575 and 2610 kb. As migrations are dependent on DNA amounts, the present sizings may be somewhat overestimated (Bernards *et al.*, 1986). Tentative estimations based on indirect arguments suggested that the size of the pseudo-autosomal region should not exceed 5 Mb (Rouyer *et al.*, 1986a). According to the present sizing, the pseudo-autosomal region represents 3-5% of the human Y chromosome and <2% of the X chromosome. Pritchard *et al.* (1987) have localized the proximal boundary of the pseudo-autosomal region between 45 and 125 kb proximal to the MIC2 HTF island. We have now observed a more distal Y-specific *NruI* site 80 kb proximal to the MIC2 HTF island, suggesting that the boundary maps 45-80 kb proximal to this HTF island.

**Comparing physical and recombination maps**

The different pseudo-autosomal loci can be positioned from the telomere to the proximal boundary along a linkage map according to their increasing linkage to TDF (Rouyer *et al.*, 1986a). When these linkage data were not accurate enough, the loci order could sometimes be completed by segregation analyses between two closely linked loci in informative families (Rouyer *et al.*, 1987). The present linkage map (see Davies *et al.*, 1988) gives the order: pter-DXYS14-DXYS20-DXYS60-DXYS28-DXYS15, DXYS59-DXYS17-MIC2-cen. The same order has been found in the present physical map (Figure 2). In addition, DXYS15 and DXYS59, which could not be separated by linkage analysis were ordered on the physical map (Figure 2).

The telomeric locus DXYS14/DXYS20 recombines with TDF at 47.4% (363 meioses analysed) in male meiosis (for a compilation of linkage data, see Weissenbach, 1988). Since no double recombination within this region has been observed to date, a mean distance per recombination unit can be

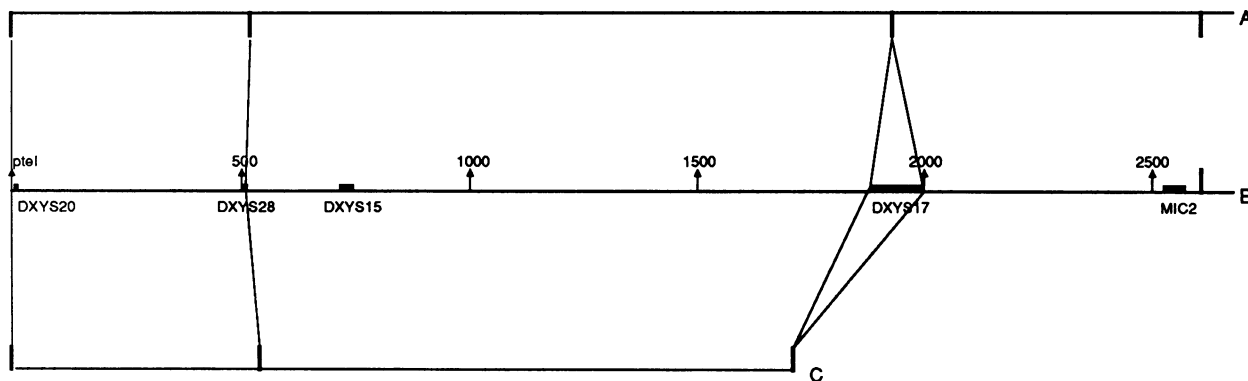


**Fig. 7.** Physical (line B) and genetic linkage maps (lines A and C) of the human pseudo-autosomal region. Loci on the genetic map A are positioned according to their linkage distance to sex (sex is assimilated to the recombination limit corresponding to the proximal pseudo-autosomal boundary), see Table V. Loci on the genetic map C are positioned according to their linkage distance to DXYS14/DXYS20.

determined for the entire region (Table V). One cM represents 55 kb in male meiosis corresponding to an 18-fold increase compared to the mean autosomal value. This 18-fold increase equates well with the 10- to 20-fold higher frequency reported in this region in male versus female meiosis (Rouyer *et al.*, 1986b; Page *et al.*, 1987). The elevated recombination frequency in male meiosis allows the comparison of the linkage and physical maps in defined intervals. We have limited this comparison to a few intervals for which recombination values were the most accurate ( $> 100$  informative meioses) (Table V). The values for each interval fluctuate between 51 and 64 kb/cM, indicating that recombination hot spots or regions of recombination inhibition (if any) cannot be noticed at this level of resolution. This is also illustrated by the superimposition of both genetic linkage and physical maps which shows no significant distortion (Figure 7) in male meiosis.

#### Distribution of undermethylated CpG dinucleotides

The most distal part of the sex chromosome short arms exhibits a very high number of undermethylated CpG dinucleotides; this can be especially appreciated through the density of restriction sites containing two CpG doublets (*MluI*, *SacII*, *NorI*, *NruI*, *BssHIII*, *SalI*). The distribution of the CpG-rich sites is not uniform; they are very dense in the 200 kb closest to the telomere and around locus DXYS28, but rather less abundant in the p<sub>tel</sub>:210–p<sub>tel</sub>:480 interval. Most of the individual variations, analysed on five 45,X Turner patients, appear essentially in the 500 kb closest to the telomere. Such an extreme density of CpG-rich sites is unprecedented in other long-range segments of the human genome, even in regions known for their high gene density (Hardy *et al.*, 1986; Lawrance *et al.*, 1987; Müller *et al.*, 1987). Though many of these sites appear in clusters, these clusters are very densely gathered and do not seem reminiscent of classical HTF islands (Bird, 1986; Brown and Bird, 1986) which are rather scattered in the genome. This extreme density of CpG restriction sites may reflect some structural features possibly related to telomeric functions. In this respect mapping of another human or mammalian telomeric region will be of interest. Though considerably smaller than chromosomal staining bands, the present CpG-rich regions may also be in some way related to the heavy isochores described by Bernardi *et al.* (1985). Other CpG-rich clusters at p<sub>tel</sub>:1300, p<sub>tel</sub>:1530, p<sub>tel</sub>:2300, p<sub>tel</sub>:2400 and p<sub>tel</sub>:2530 are scattered in the rest of the region. They appear more typical of classical HTF islands, and are therefore likely to label gene locations (Bird *et al.*, 1985). Differences in methylation patterns between sequences from the active and inactive X have been reported in several instances (reviewed in Monk, 1986).

Undermethylation in HTF islands has been correlated with X-linked gene activity (Yen *et al.*, 1984; Keith *et al.*, 1986; Toniolo *et al.*, 1988). Methylation pattern differences should be noticeable at the level of CpG-rich cutting sites in HTF islands observed by pulsed field analyses. It is, for instance, expected that most X-located HTF islands will be more sensitive to cleavage in 45,X than in 48,XXXX peripheral lymphocytes. Such a difference is, however, not observed between these genotypes in the pseudo-autosomal region. This is in agreement with similar observations on the MIC2 HTF island (Goodfellow *et al.*, 1987), a gene known to escape X-inactivation (Goodfellow *et al.*, 1984). This

suggests that if pseudo-autosomal HTF islands are associated with transcribed regions, these genes also escape inactivation as predicted by Lyon (1962).

## Materials and methods

#### Probes

362A (locus DXYS20) is a probe detecting a VNTR (see Weissenbach *et al.*, 1987) spanning 40–60 kb, and is located 10–15 kb proximal to 29C1 (Rouyer *et al.*, 1986b). 29C1 (locus DXYS14) has been mapped at ~10 kb from the Xp/Yp telomere (Cooke *et al.*, 1985). Probe 362A is thus located 20–30 kb proximal to the telomere and is homologous to 29A24 (Cooke and Smith, 1986) and pDP230 (Page *et al.*, 1987). Locus DXYS60 is defined by probe U7A and maps between loci DXYS20 and DXYS28 (Rouyer *et al.*, 1987). Probe pDP411 defines locus DXYS28 (Page *et al.*, 1987). Loci DXYS59 and DXYS15 (probes 68A and 113D respectively) have not been resolved by family analysis to date (M.C. Simmler *et al.*, unpublished). Probe 601 defines locus DXYS17 (Rouyer *et al.*, 1986a,b). Several probes from the MIC2 gene were used for this study (Goodfellow *et al.*, 1986). They map either distal (probe p44A, personal communication and gift from P. Goodfellow) or proximal (probe 19B) to the HTF island occurring at the distal end of the gene (Pritchard *et al.*, 1987).

#### DNA sources and digestions

Peripheral lymphocytes from five 45,X Turner, one 46,XX, one 46,XY and one 48,XXXX individuals, purified using Ficoll–Paque (Pharmacia), and a 49,XYYYY EBV-transformed lymphoblastoid cell line (CHM062) were used as DNA sources.

In brief,  $8 \times 10^5$  cells were included in 60- $\mu$ l low melting agarose blocks. DNA was prepared according to Hermann *et al.* (1987). Blocks were stored in 0.5 M EDTA, pH 8, and equilibrated in the digestion buffer prior to use. Blocks were incubated with 20 U of enzyme for 7–15 h. Blocks submitted to double digestions were reequilibrated with the appropriate buffer.

#### Pulsed field gel electrophoresis

Orthogonal field gel electrophoresis was performed in an LKB pulsaphore apparatus. Agarose gels (1%) were run in 0.25  $\times$  TBE, 200 V at 15°C for 62–68 h; switching times of 60 s, 165 s and 240 s were used to separate molecules up to 600 kb, 1100 kb and 1500 kb respectively. Separations up to 4.5 Mb were achieved in 0.7% agarose gels run for 5 days in 0.5  $\times$  TBE, 150 V at 15°C with a switching time of 30 min, followed by another 24-h run with a switching time of 165 s. Contour-clamped homogeneous electric field (CHEF) gel electrophoresis was performed in apparatus as designed by Chu *et al.* (1986). Agarose gels (1%) were run in 0.5  $\times$  TBE, 100 V at 15°C for 42–45 h; switching times of 70 s, 130 s and 240 s were respectively used to separate molecules up to 600 kb, 1000 kb and 1600 kb. Agarose gels (0.7%) were run for 6 days in 0.5  $\times$  TBE, 50 V at 15°C with a 45-min switching time to separate molecules up to 6 Mb. After staining with ethidium bromide, gels were exposed to short wavelength UV light for 2 min and soaked in 0.25 N HCl for 2  $\times$  15 min followed by 0.4 N NaOH for 2  $\times$  15 min. DNA was transferred to nylon membranes (GeneScreen, NEN) in 0.4 N NaOH for 40 h. Filters were neutralized, baked for 2 h at 80°C and hybridized according to Church and Gilbert (1984).

Genomic fragments were sized by comparison with  $\lambda$  concatemeres (prepared according to Hermann *et al.*, 1987) and with chromosomes from *Saccharomyces cerevisiae*, strain AB972 (prepared according to Carle and Olson, 1985), *Plasmodium chabaudi* and *P. falciparum* (a gift of G. Langsley) and *Schizosaccharomyces pombe* (prepared according to Smith *et al.*, 1987). The largest *P. chabaudi* and *P. falciparum* chromosomes were 2100 kb and 3200 kb (G. Langsley, personal communication). The sizes of all fragments have been determined at least twice. Because of variations in DNA amounts in different migrations, reported values are still approximate (Bernards *et al.*, 1986).

## Acknowledgements

We wish to thank Denise Barlow, Suzanne Carlson, François Caron, Brigitte Gicquel-Sanzey and Gordon Langsley for their help and advice, Peter Goodfellow and David Page for DNA probes, Bernard Noel for blood samples, Yannick Archambaud for the construction of CHEF apparatus, Mike Mitchell for reading this manuscript and Pierre Tiollais for his encouragement and support.

## References

- Bernardi, G., Olofsson, B., Filipinski, J., Zerial, M., Salinas, J., Cuny, G., Meunier-Rotival, M. and Rodier, F. (1985) *Science*, **228**, 953–958.
- Bernards, A., Kooter, J.M., Michels, P.A.M., Moberts, R.M.P. and Borst, P. (1986) *Gene*, **42**, 313–322.
- Bird, A.P. (1986) *Nature*, **321**, 209–213.
- Bird, A.P., Taggart, M., Frommer, M., Miller, O.J. and Macleod, D. (1985) *Cell*, **40**, 91–99.
- Brown, W.R.A. and Bird, A.P. (1986) *Nature*, **322**, 477–481.
- Burgoyne, P.S. (1982) *Hum. Genet.*, **61**, 85–90.
- Buckle, V., Mondello, C., Darling, S., Craig, I.W. and Goodfellow, P.N. (1985) *Nature*, **317**, 739–741.
- Carle, G.F. and Olson, M.V. (1985) *Proc. Natl. Acad. Sci. USA*, **82**, 3756–3760.
- Chandley, A.C., Goetz, P., Hargreave, T.B., Joseph, A.M. and Speed, R.M. (1984) *Cytogenet. Cell Genet.*, **38**, 241–247.
- Chu, G., Vollrath, D. and Davis, R.W. (1986) *Science*, **234**, 1582–1585.
- Church, G.M. and Gilbert, W. (1984) *Proc. Natl. Acad. Sci. USA*, **81**, 1991–1995.
- Cooke, H.J. and Smith, B.A. (1986) *Cold Spring Harbor Symp. Quant. Biol.*, **51**, 213–219.
- Cooke, H.J., Brown, W.A.R. and Rappold, G. (1985) *Nature*, **317**, 688–692.
- Darling, S.M., Goodfellow, P.J., Pym, B., Banting, G.S., Pritchard, C. and Goodfellow, P.N., (1986) *Cold Spring Harbor Symp. Quant. Biol.*, **51**, 205–212.
- Davies, K., Mandel, J.L., Weissenbach, J. and Fellous, M. (1988) *Cytogenet. Cell Genet.*, in press.
- Evans, E.P., Burtenshaw, M.D. and Cattanaach, B.M. (1982) *Nature*, **300**, 443–445.
- Ferguson-Smith, M.A. (1965) *J. Med. Genet.*, **2**, 142–155.
- Goodfellow, P.N., Pym, B., Mohandas, T. and Shapiro, L.J. (1984) *Am. J. Hum. Genet.*, **36**, 777–782.
- Goodfellow, P.J., Darling, S.M., Thomas, S.N. and Goodfellow, P.N. (1986) *Science*, **234**, 740–743.
- Goodfellow, P.J., Darling, S., Banting, G., Pym, B., Mondello, C. and Goodfellow, P.N. (1987) *Development*, **101** (Suppl.), 119–125.
- Harbers, K., Soriano, P., Müller, U. and Jaenisch, R. (1986) *Nature*, **324**, 682–685.
- Hardy, D.A., Bell, J.I., Long, E.O., Lindsten, T. and McDevitt, H.O. (1986) *Nature*, **323**, 453–455.
- Herrmann, B.G., Barlow, D.P. and Lehrach, H. (1987) *Cell*, **48**, 813–825.
- Keitges, E., Rivest, M., Siniscalco, M. and Gartler, S.M. (1985) *Nature*, **315**, 226–227.
- Keitges, E.A., Schorderet, D.F. and Gartler, S.M. (1987) *Genetics*, **116**, 465–468.
- Keith, D.H., Singer-Sam, J. and Riggs, A.D. (1986) *Mol. Cell. Biol.*, **6**, 4122–4125.
- Koller, P.C. and Darlington, C.D. (1934) *J. Genet.*, **29**, 159–173.
- Lawrance, S.K., Smith, C.L., Srivastava, R., Cantor, C.R. and Weissman, S.M. (1987) *Science*, **235**, 1387–1390.
- Lyon, M.F. (1963) *Am. J. Hum. Genet.*, **14**, 135–148.
- Monk, M. (1986) *BioEssays*, **4**, 204–208.
- Müller, U., Stephan, D., Philippsen, P. and Steinmetz, M. (1987) *EMBO J.*, **6**, 369–373.
- Page, D.C., Bieker, K., Brown, L.G., Hinton, S., Leppert, M., Lalouel, J.M., Lathrop, M., Nyström-Lahti, M., de la Chapelle, A. and White, R. (1987) *Genomics*, **1**, 243–256.
- Pritchard, C.A., Goodfellow, P.J. and Goodfellow, P.N. (1987) *Nature*, **328**, 273–275.
- Rouyer, F., Simmler, M.C., Johnsson, C., Vergnaud, G., Cooke, H. and Weissenbach, J. (1986a) *Nature*, **319**, 291–295.
- Rouyer, F., Simmler, M.C., Vergnaud, G., Johnsson, C., Levilliers, J., Petit, C. and Weissenbach, J. (1986b) *Cold Spring Harbor Symp. Quant. Biol.*, **51**, 221–228.
- Rouyer, F., Simmler, M.C., Page, D.C. and Weissenbach, J. (1987) *Cell*, **51**, 417–425.
- Singh, L. and Jones, K.W. (1982) *Cell*, **28**, 205–216.
- Simmler, M.C., Rouyer, F., Vergnaud, G., Nyström-Lahti, M., Ngo, K.Y., de la Chapelle, A. and Weissenbach, J. (1985) *Nature*, **317**, 692–697.
- Smith, C.L., Matsumoto, T., Niwa, O., Klco, S., Fan, J.B., Yanagida, M. and Cantor, C.R. (1987) *Nucleic Acids Res.*, **15**, 4481–4489.
- Soriano, P., Keitges, K.A., Schorderet, D.F., Harbers, K., Gartler, S.M. and Jaenisch, R. (1987) *Proc. Natl. Acad. Sci. USA*, **84**, 7218–7220.
- Toniolo, D., Martini, G., Migeon, B.R. and Dono, R. (1988) *EMBO J.*, **7**, 395–406.
- Weber, B., Weissenbach, J. and Schempp, W. (1987) *Cytogenet. Cell Genet.*, **45**, 26–29.
- Weissenbach, J. (1988) *Proc. R. Soc. Ser. B*, in press.
- Weissenbach, J., Levilliers, J., Petit, C., Rouyer, F. and Simmler, M.C. (1987) *Development*, **101** (Suppl.), 67–74.
- Yen, P.H., Patel, P., Chinault, A.C., Mohandas, T. and Shapiro, L.J. (1984) *Proc. Natl. Acad. Sci. USA*, **81**, 1759–1763.

Received on April 14, 1988